Impact of annealing treatment on the microstructural-dependent mechanical properties of a cold-rolled Fe-Co-10V alloy

M.R. Kamali[a], A.R. Mashreghi[a,] *, L.P. Karjalainen[b], S. Hasani[a], V. Javaheri[b],

M. Seiyedbeigi[c], J. Kömi[b]

[a]*Department of Mining and Metallurgical Engineering, Yazd University, Yazd, Iran*

[b]*Centre for Advanced Steels Research, University of Oulu, P.O. Box 4200, FI-90014 Oulu, Finland*

[c]*Department of Materials Engineering, Malek Ashtar University of Technology, Isfahan, Iran*

Abstract

Various contributors have been suggested so far to explain the variation of mechanical properties of Fe-Co-V magnetic alloys, but a comprehensive understanding is still lacking. In the present study, the variation of hardness, tensile yield strength (YS), and elongation at room temperature were determined for an 86% cold-rolled Fe-50Co-10V (wt.%) alloy after annealing at the temperature range of 300–1050 °C for holding times from 10 to 240 min. The potential contributing factors were analyzed and discussed. Detailed microstructural evolution and magnetic properties have been reported earlier for this alloy. The results showed an increase in hardness and YS but a reduction in elongation after annealing at temperatures between 450 and 550 °C for all holding times. The activation energy of the contributing process in increasing the hardness after annealing between 300–550 °C was 132–144 kJ/mol, being a typical value for the ordering transition in ferrite in Fe-Co and Fe-Co-2V alloys. The YS increased up to an annealing temperature of 450 °C, followed by a decreasing trend at higher annealing temperatures even in the ordered state, obviously due to i) the recovery and recrystallization of ferrite, ii) decreasing the number of $(Co,Fe)_3V$ precipitates and iii) increasing fraction of retained austenite. The elongation decreased to nil

after annealing at 450–550 °C, but it was improved even in the ordered state at 600 °C and above due to the same factors which decreased the YS. The intergranular failure mode after annealing below 600 °C converted to ductile mode at 650 °C. Considering the combination of mechanical and magnetic properties, the annealing treatment at 650 °C for 10 min can be recommended for this alloy, providing high YS, a few percent elongation, and high magnetic hardness.

Keywords: Fe-Co-V alloys, Annealing, Hardness, Yield strength, Ductility, Ordering, Microstructure

1. Introduction

Iron-cobalt-vanadium alloys can be processed to exhibit excellent magnetic properties for use in high-performance power generation applications such as the rotors and stators of aircraft integrated power units [1]. For these kinds of applications, although a high level of strength is essential for rotors to support the centrifugal forces generated at high rotational speeds, appropriate ductility is also required to prevent early failure during the assembling or subsequent working and maintenance stage. Several metallurgical phenomena such as ordering transition, recovery and recrystallization, precipitation, and austenite transformation take place during annealing of these cold-rolled alloys, as were recently investigated in detail by the present authors for an Fe-50Co-10V (hereafter the concentrations are in wt.%, if not differently mentioned) alloy [2,3]. In principle, all the above-mentioned microstructural changes and phase evolutions can significantly affect the mechanical and magnetic properties of these alloys. Regarding the magnetic properties, a comprehensive study was conducted recently [4]. However, mechanical properties, particularly in alloys with a high vanadium content seem to have attracted less attention yet and some contradictions concerning the effective parameters on these properties exist in the literature. Therefore, the present study

was focused on room temperature mechanical properties achieved by various annealing treatments, and their connection with the microstructure was analyzed.

There are various studies on mechanical properties of Fe-Co and Fe-Co-V alloys with low vanadium contents suggesting different metallurgical factors affecting the final mechanical properties [5–11]. For example, effects of both long- and short-range order on mechanical properties of low vanadium Fe-Co based alloys have been reviewed and discussed by Sundar and Deevi [12] as well as by Sourmail [13]. Stoloff and Davis [11] by investigating an Fe-Co–2V (at%) alloy reported that the strength of the alloy reaches a maximum at an intermediate degree of order at 710 °C, slightly below the critical order-disorder transition temperature (*Tc*). For an Fe-Co-7.15V alloy, Hasani et al. [14] related an increase in hardness and strength of the alloy to the disorder to order transition which was considered as the most effective contributor to the mechanical properties.

Sourmail [15] by comparing the data obtained in various studies, particularly by Thornburg [16] and Hailer [1], concluded that the coercivity and the strength of an Fe-Co-2V after annealing treatment can be explained quantitatively based barely on grain size variation rather than by postulating variation in the extent of recrystallization or degree of order. He also attributed the sharp variations in magnetic and mechanical properties of the alloy around the T_c to significant grain growth occurring around this temperature. Nabi et al. [8] determined the YS of a cold-rolled and annealed Fe-Co-2V-0.04Nb alloy based on an experimental Hall–Petch relationship as a function of boundary spacing of ferrite grains in both the ordered and disordered conditions.

However, the main problem is that the ductility of the ordered structure is very low, but there are different opinions concerning the contributing factor. For an Fe-Co-2V alloy, the nil-ductility temperature (corresponding to a YS equal to fracture stress) was found to be

sensitive to the state of order and ferrite grain size [17]. According to Thornburg [16], the maximum elongation was obtained for an Fe-49Co-2V alloy at around 670 °C, where there were fine 10–20% recrystallized grains. However, in an Fe-49.6Co-7.15V alloy, austenite formation was proposed as solely responsible for increasing the ductility after annealing above 450 °C and below 750 °C [14].

As can be realized from the above-mentioned studies, various factors, often a single one, have been suggested so far to explain the variation of mechanical properties. This is more acceptable in the case of Fe-Co-2V alloys where those phenomena can take place at different temperature ranges, but in the case of 7–10 % V alloys where microstructural changes occur simultaneously, the situation can be more complicated. Hence, to clarify this situation, the relation of mechanical properties and the microstructural evolution after various annealing treatments was systematically investigated for a 10 % V alloy. Finally, the optimal combination of mechanical and magnetic properties achievable by annealing is briefly considered.

2. Experimental methodology

2.1. Test material and thermal cycles

The material used in this study was prepared in a vacuum arc furnace from pure charge elements. The chemical composition of the produced alloy was 49.8 % Co, 40.1 % Fe, 9.96 % V, and balance other elements, determined by the inductively coupled plasma mass spectrometry. The cast ingots were homogenized at 1200 °C for 10 h to modify the as-cast structure. Afterward, hot rolling in the temperature range of 950–850 °C following by 86% cold rolling to a final thickness of 0.14 mm was carried out on the sheets. Then, annealing treatments in the temperature range of 300–1050 °C and durations of 10–240 min were

performed on cold-rolled thin sheets in a vacuum tube furnace with a heating and cooling rate of 5 and 10 °C/s, respectively.

2-2. Mechanical properties

Hardness was measured using a Duramin-A300 (Struers) tester under a low 10 N load owing to the small thickness of samples. The area of 10*10 mm of the sheet surface and an average of 10 measurements with a 2 mm distance between each point were adopted.

Tensile tests were carried out using a Zwick/Roell Z100 machine at room temperature by an initial strain rate of 0.008 s^{-1}. The dimensions of the sub-size tensile test specimens cut in the rolling direction are shown in Fig. 1. Three tensile specimens were tested for each condition and the average was reported as the result.

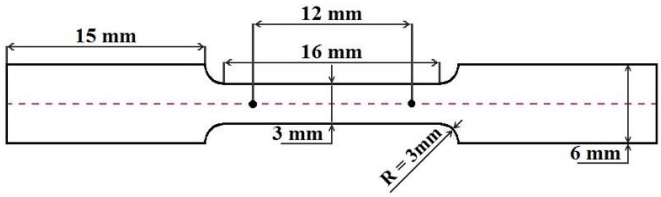

Fig. 1. Dimensions of sub-size tensile test specimen used in experiments.

2.3. Microstructural characterization

Microstructural evolution in this alloy has been reported earlier [2,3], but due to its high importance, some essential details have been given here. After the standard metallographic sample preparation, microstructural features of the polished samples and fracture surface were analyzed using a Sigma Zeiss field-emission scanning electron microscope (FESEM) equipped with an electron backscatter diffraction (EBSD) unit (EDAX Apollo X). An accelerating voltage of 5 kV and 15 kV, as well as a working distance of 5 mm and 15 mm, were employed for SEM imaging and EBSD, respectively. A step size of 30 nm was used in

EBSD runs and data analyses were performed using the EDAX-OIM analysis software (TSL).

A DIL 805 A/D dilatometer was employed to study the dimensional changes related to the phenomena that occur during the heating and cooling of the studied material. A cylindrical sample with a diameter of 4 mm and a height of 10 mm was prepared for dilatometric tests. The peak temperature of 1000 °C, the heating and cooling rate of 10 °C/min and holding time of 15 min at maximum temperature were selected as the testing cycle under a continuous flow of argon gas.

For accurate phase analysis, a Rigaku Smart Lab 9 kW X-ray diffractometer with a Co rotating anode operated at 40 kV and 135 mA in the back-reflection mode and a step size of 0.02° was utilized. In order to remove the effect of texture on X-ray reflections, measurements were performed using an average of seven different angles.

TEM imaging was conducted using a 200 kV energy filtered scanning transmission electron microscope (JEOL JEM- 2200FS EFTEM/STEM). Thin foils for TEM analyses were prepared using the focused ion beam (FIB) technique. Also, imaging and elemental mapping were performed using bright field imaging mode in scanning TEM (STEM) mode with a JEOL Dry SD100GV EDS detector.

2.4. Magnetic properties

A vibrating sample magnetometer device (VSM, MDKB model) with a maximum field intensity of up to 1 tesla at room temperature was employed to assess the magnetic properties. A wire cut machine was used to prepare the VSM specimens with dimensions of 5*5*0.14 mm.

3. Results

3.1. Microstructural evolution and phase transformations

Comprehensive investigations of microstructural evolutions and phase transformations during annealing of the studied material have been carried out by the same authors and detailed results can be found in Refs. [2,3]. However, owing to the close dependence of mechanical properties on microstructural features, a brief review of those observations is presented here for readers' convenience.

During annealing of the cold rolled alloy, several important phenomena including ordering transformation, recovery and recrystallization, precipitation, and austenite formation take place in very close temperature intervals. Some of them are observed in the dilatometric curve, presented in Fig. 2(a) and comprehensively discussed in Ref. [3]. Importantly, the start of the ordering process in the ferrite (martensite) is seen at around 350 °C. The XRD patterns in special degree ranges are plotted in Fig. 2(b-d). It is reported that the superlattice diffraction peak due to the ordering transition in the ferrite phase is visible at $2\theta = 36.5°$ concerning the (100) planes [18]. Hence, the superlattice reflections in the XRD pattern in Fig. 2(b) indicate the appearance of the ordering at 500 °C during 120 min followed by its intensification up to 600 °C and then weakening, until vanishing at 750 °C.

Besides, the precipitation of the HCP phase (γ_2) causes the reflections at $2\theta = 48.5°$ (Fig. 2(c)) and $2\theta = 56.5°$ (not shown here) appeared by annealing at 500 °C for 120 min, intensified at 550 °C but weakened at higher annealing temperatures and finally disappeared at 700 °C. Reflections of the austenite phase (γ) became visible after annealing at 550 °C for 120 min and the height of (220) peak, shown in Fig. 2(c)), was amplified toward higher annealing temperatures until the maximum at 750 °C. Annealing at 800 °C for 120 min decreased the intensity of the austenite peak, and after annealing at 850 °C, no trace of

austenite reflection remained, whereas the microstructure was fully martensitic at room temperature.

Further evidences of the formation of the austenite phase were obtained by the EBSD technique [3]. Examples of EBSD phase analysis are shown in Fig. 3. As seen, the microstructure was still ferritic (martensite) in the sample annealed at 500 °C for 60 min, but a considerable amount of austenite with a very fine grain size was formed at 650 °C, mostly along the high angle grain boundaries of ferrite. Actually, EBSD analysis revealed that the formation of austenite initiated at 550 °C in agreement with the XRD results [3]. The maximum amount of austenite is achieved after annealing at 750 °C (Fig. 3(c)) and a tiny fraction is remained after annealing at 800 °C, in agreement with the XRD patterns.

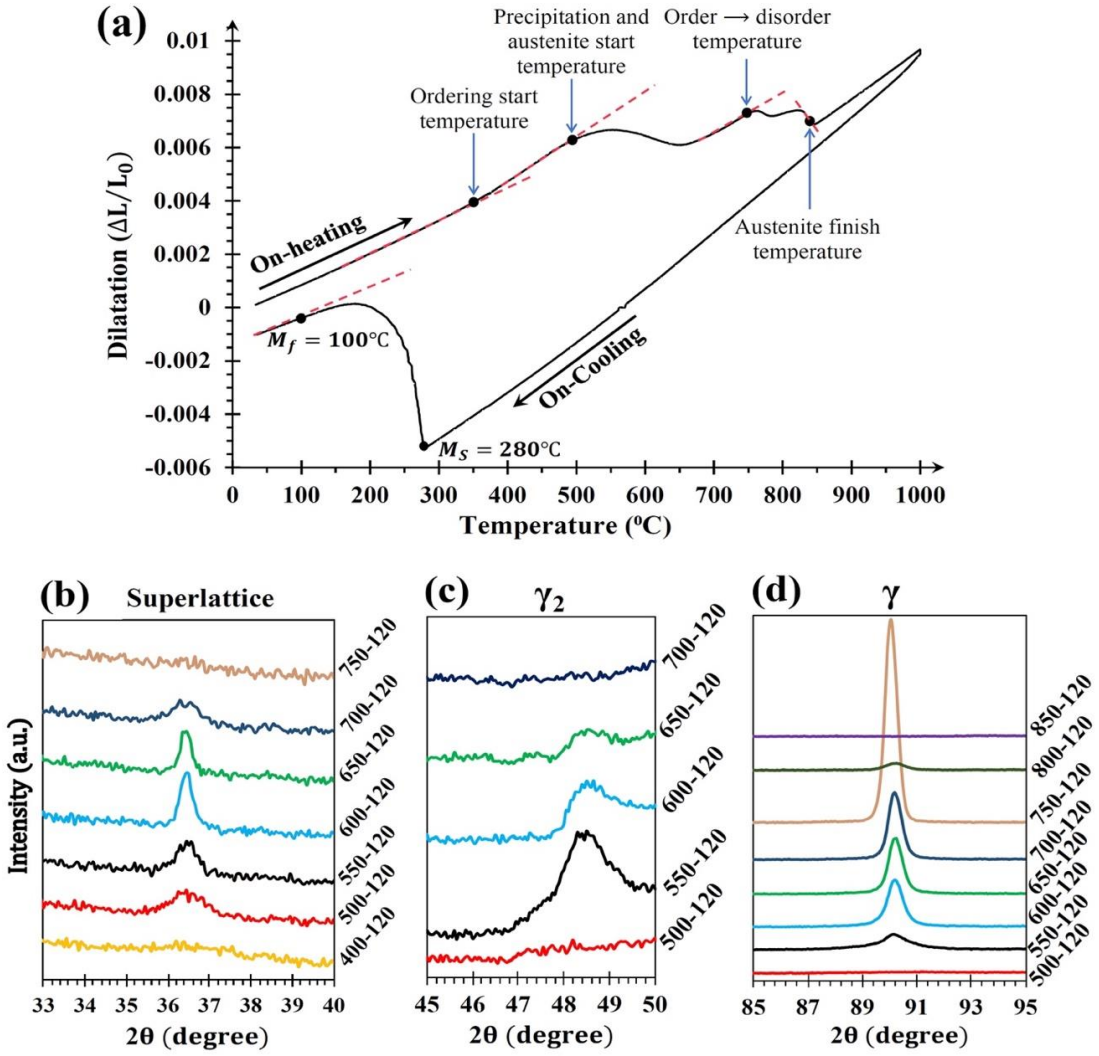

Fig. 2. Ranges of phase transformations and microstructural changes. Dilatation revealing ordering, precipitation, and formation of austenite on heating and martensite upon cooling in (a). XRD revealing ordering in (b), γ_2 precipitates in (c), and austenite (γ) in (d) after annealing at various temperatures for 120 min.

It must be noted that during the ordering, precipitation, austenite transformation, recovery, and static recrystallization of cold-rolled ferrite (martensite) can take place simultaneously. The progress of softening was investigated earlier employing various EBSD techniques [3]. It was found that the continuous recrystallization begins at 600 °C within 60 min through the conversion of low-angle grain boundaries to high-angle grain boundaries, but the kinetics of recrystallization in the ordered ferrite was very slow. The early stage of recrystallization can be seen as the presence of small grains in Fig. 3(b). At 750 °C, 83% of ferrite has

recrystallized within 60 min, though this is difficult to see in a phase map in Fig. 3(c), for this requires Image Quality, Kernel Average Misorientation and Grain Orientation Spread techniques, employed in an early work [3].

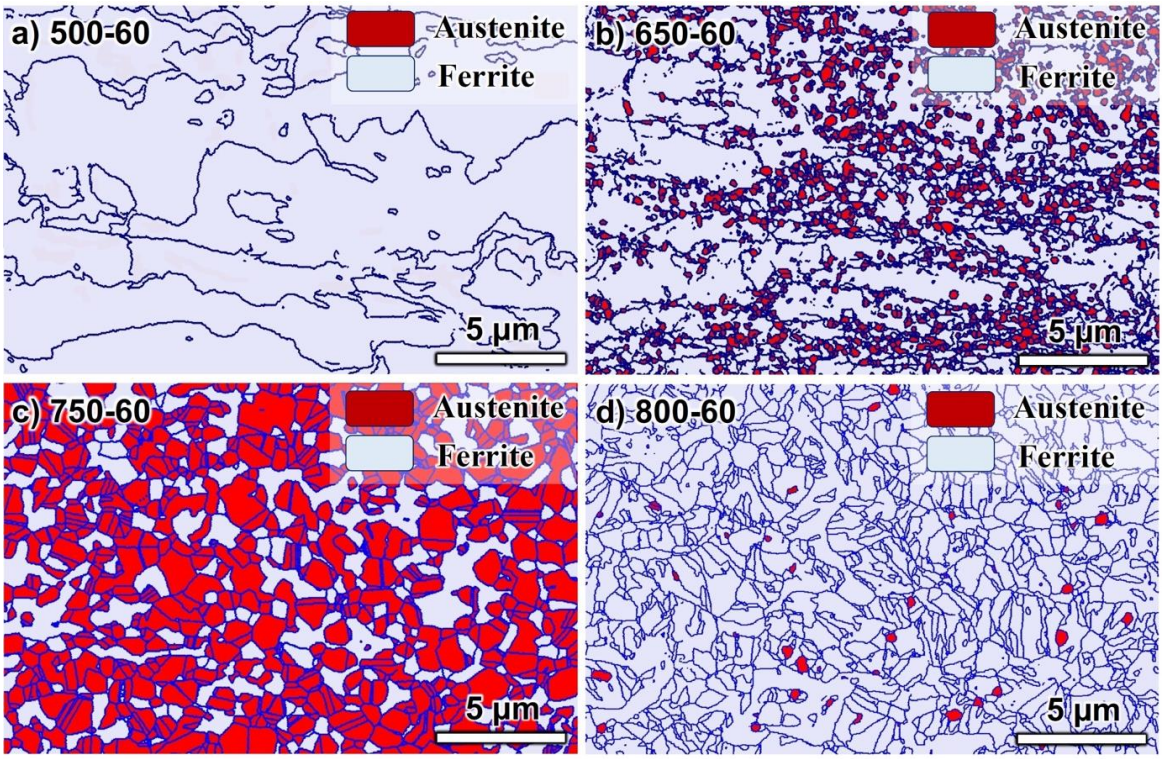

Fig. 3. EBSD phase maps overlapped high-angle grain boundary maps of annealed samples for 60 min at various temperatures (a, b, c, and d).

As can be noticed from Fig. 3, the fraction of the austenite phase increased significantly between 650 and 750 °C, but then it almost disappeared after annealing at 800 °C while new martensite formed during cooling replaced it. This is connected with the stability of the austenite phase depending on its vanadium content. TEM is needed to characterize tiny γ_2 precipitates and the analysis of chemical compositions of the ordered ferrite and austenite phases requires TEM-EDS examinations. Such studies were performed in previous work [3]. An example of the microstructure after annealing at 650 °C for 60 min is shown in Fig. 4(a). Rod-shaped phase (γ_2), with the composition of $(Co,Fe)_3V$ and HCP crystal structure, being

rich from vanadium and poor from iron, exists in the microstructure in addition to V-depleted ordered ferrite and V-enriched ordered austenite [3]. Those precipitates decreased by increasing the annealing temperature and entirely vanished at 750 °C, where the microstructure only consisted of disordered austenite and disordered ferrite, as seen in Fig. 4(b).

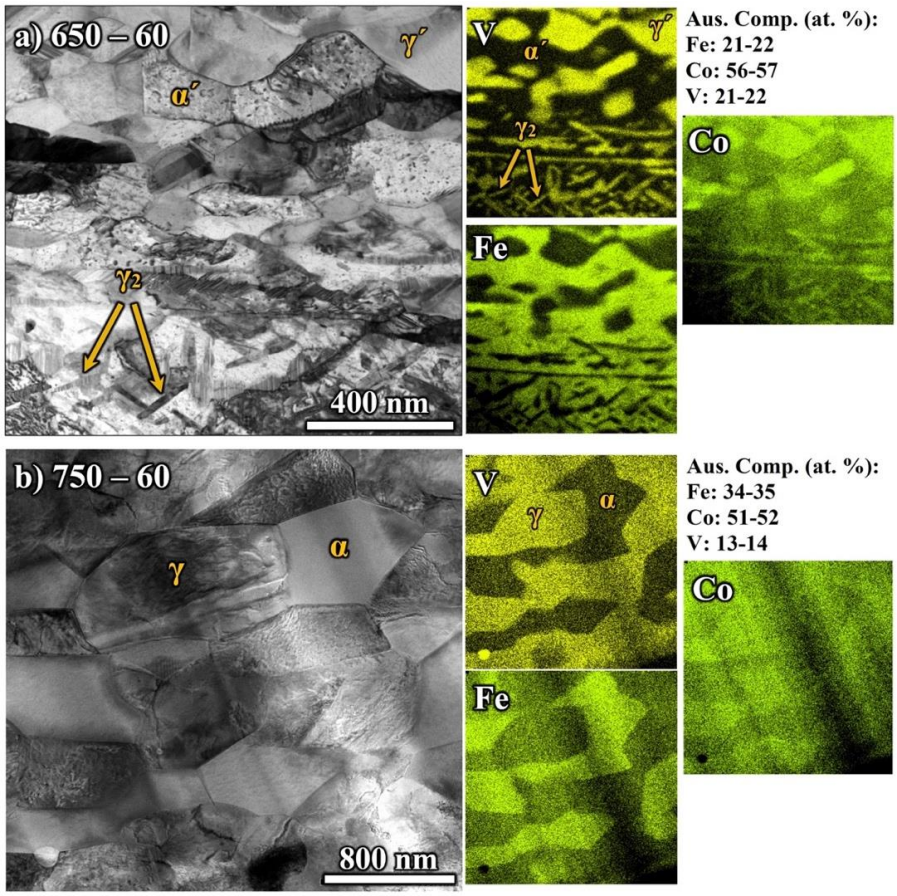

Fig. 4. TEM images of annealed samples for 60 min at 650 ºC (a) and 750 ºC (b) along with elemental maps showing the distribution of elements in various phases. α′, γ′, γ2, α and γ represent ordered ferrite, ordered austenite, precipitates, disordered ferrite, and disordered austenite respectively.

3.2. Mechanical properties

3.2.1. Hardness evolution

The initial hardness of the cold-rolled martensitic sheet was 310 ± 15 HV. The hardness of the samples (at room temperature) after annealing in the temperature range of 200–1050 °C for various holding times is plotted in Fig. 5. As seen, the sharp increase in hardness takes place from 320 ± 15 HV concerning the annealing temperature of 200 °C, up to 740–808 (± 40) HV achieved at annealing peak temperatures between 500 and 600 °C, depending on the annealing duration. The hardness peak is followed by a steep drop to a level of 220–228 (± 10) HV by further increasing the annealing temperature up to 750 °C for different soaking times. A tiny subsidiary peak seems to appear at 800 °C. After annealing at and above 850 °C, the hardness level is quite constant, though a small reduction owing to higher temperatures and longer durations.

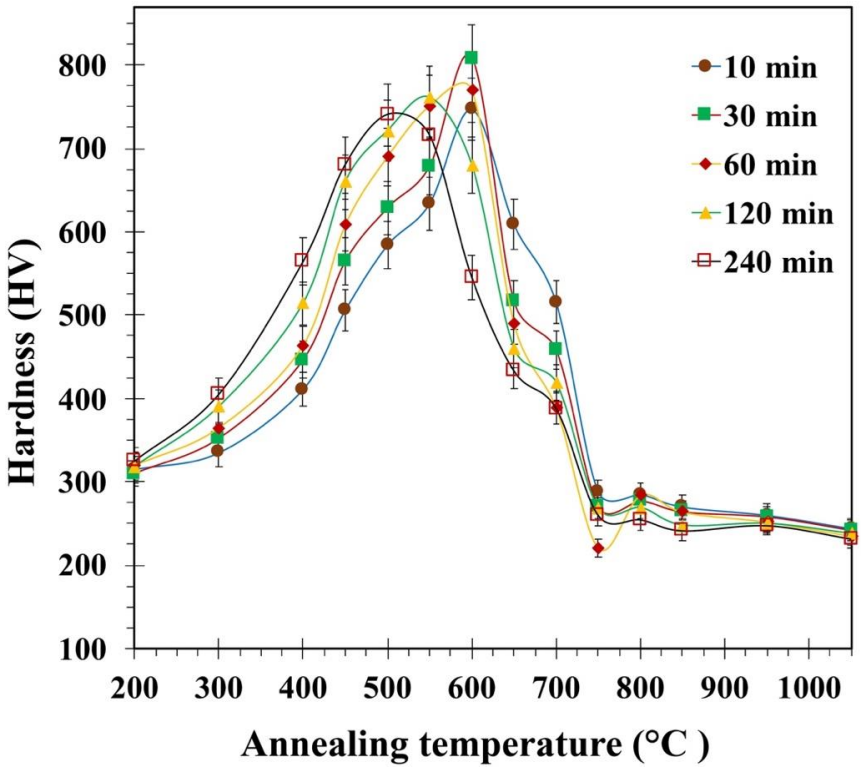

Fig. 5. Variation of hardness after various annealing conditions. (Error bars was added)

3.2.2. Tensile properties

Numerous tensile tests were carried out to investigate variations in mechanical properties of the cold-rolled alloy as a result of annealing under various conditions. For better clarification, the curves are presented in three figures (note the different scales on the X-axis); cold-rolled specimen and annealed samples until 500 °C, where the precipitation and austenite formation have no progress yet and only the ordering transition occurred, are shown in Fig. 6(a). Then samples were annealed at 550 °C and above but below T_c, where the softening of ferrite, austenite formation, precipitation, and ordering are taking place concurrently, given in Fig. 6(b). Finally, the samples annealed at temperatures above T_c, i.e., in the disordered region, are presented in Fig. 6(c).

Variations of the yield strength (0.2% offset stress) or fracture stress and elongation as a function of annealing temperature for durations of 1, 2, and 4 h are plotted in Figs. 7(a) and 7(b), respectively. According to Fig. 7(a), the YS increases from 1.5 GPa to 2.6–2.8 GPa due to the increased annealing temperature from 200 °C to 450 °C, followed by a slight drop to 2.1–2.4 GPa after annealing at 550 °C. A tiny increment is obtained by annealing at 600 °C but following by a continuous reduction up to 750 °C, before an almost constant YS level of 0.9 GPa after annealing above this temperature. It must be noted that at the temperature range 450–550 °C the fracture took place before any plastic yielding (see Fig. 6), so the data points are for the fracture stress instead of YS in this range, as indicated by hollow markers in Fig. 7(a). This will be discussed later.

The cold-rolled alloy exhibits high strength but low ductility (fracture elongation ≈ 2%) due to martensitic structure and 86% cold rolling. However, with raising the annealing temperature, the elongation still decreased, as seen in Fig. 7(b). At annealing temperatures of 450, 500, and 550 °C, the alloy became entirely brittle, and fracture took place before any plastic yielding. Further increasing the annealing temperature from 600 °C to 650–700 °C led

to increasing the elongation. Annealing above T_c, i.e., at 750 °C, resulted in distinct improvement, dependent on holding time so that the maximum elongation around 27% was reached for the shortest holding time of 60 min. The elongation, however, decreased back down to 5% after annealing at 800 and 850 °C, obviously being connected with the martensitic structure formed from unstable austenite upon cooling.

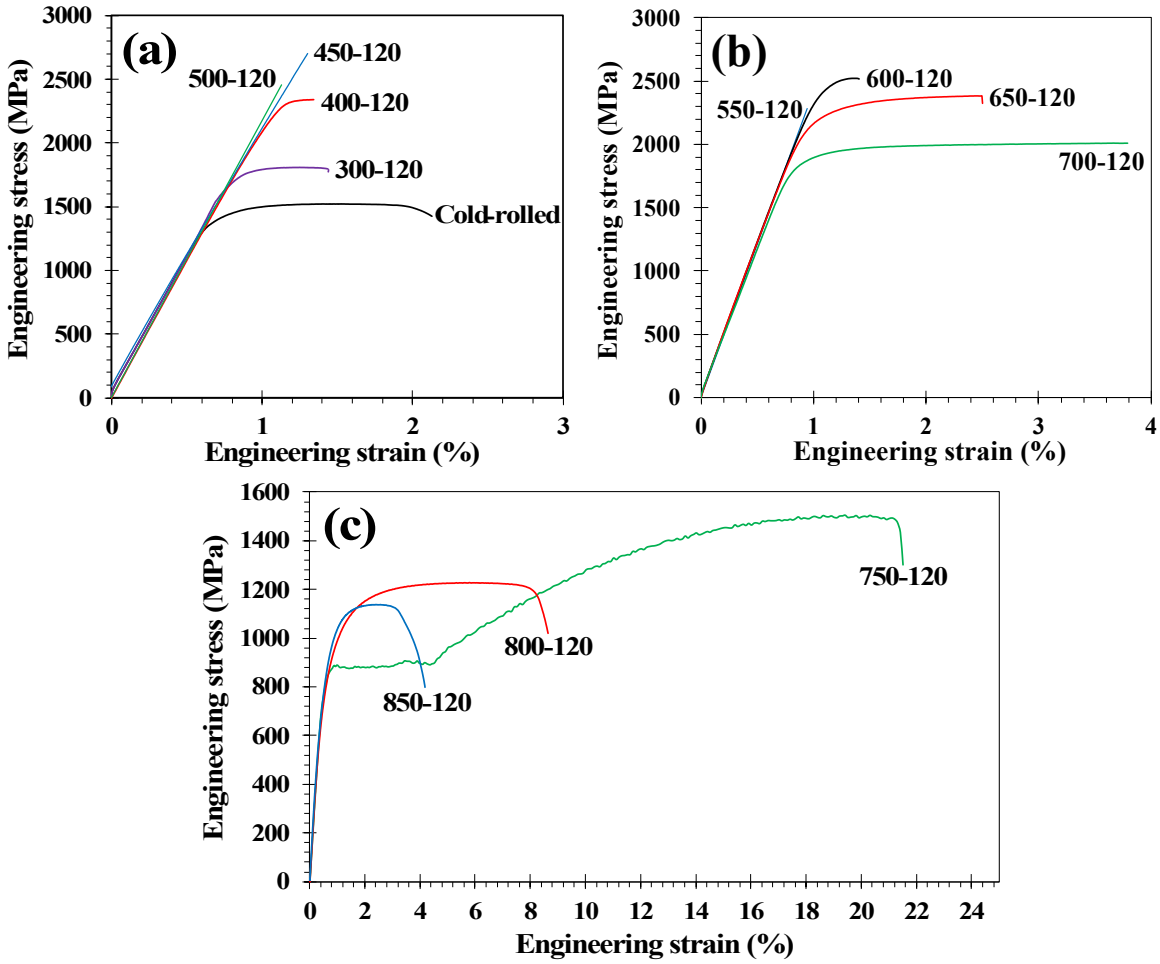

Fig. 6. Engineering stress-strain curves of samples annealed at different temperatures for 120 min. Cold-rolled and annealed at 300–500 °C (a), 550–700 °C (b), and 750–850 °C (c).

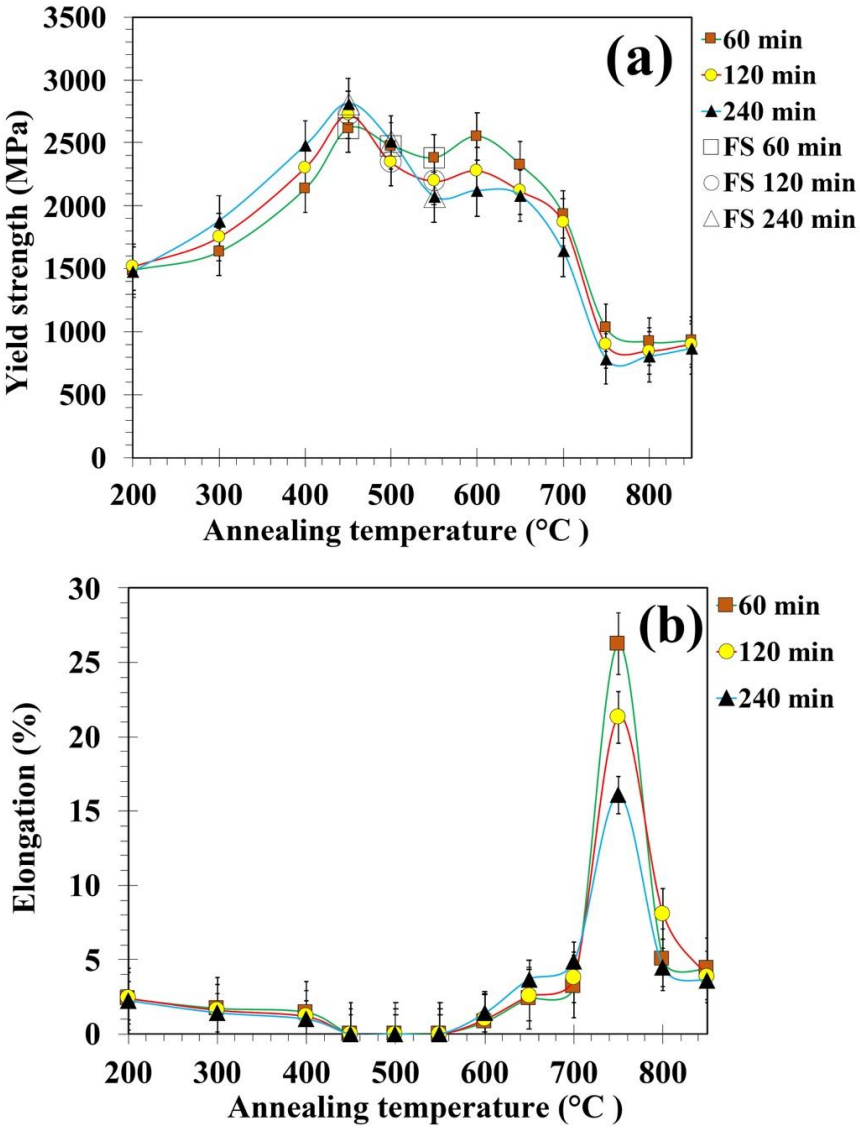

Fig. 7. Variations of yield strength and fracture stress (a) and elongation (b) of the samples annealed under various conditions. FS = fracture stress. (Error bars was added)

3.2.3. Fracture modes

To understand better the ductility variation, fracture surfaces of tensile strained samples were examined, and examples are shown in Fig. 8, for the cold-rolled specimen, annealed for 60 min at 500 °C in the ordered condition (500-60; elongation ≈ 0 %), at 650 °C in the ordered condition (650-60; elongation ≈ 2.5 %) and at 750 °C in the disordered condition with the highest elongation (750-60; elongation ≈ 26.3 %). It is seen that the failure mode changed

from the ductile mode in the cold-rolled condition (Fig. 8(a)) to the brittle cleavage mode with numerous micro-cracks, indicated by arrows in Fig. 8(b), between flattened (non-recrystallized) grains after annealing at 500 °C. Further increasing the annealing temperature to 650 °C led to the fracture surface including very fine dimples as a sign of ductile failure, despite the existence of the ordered state at this temperature (Fig. 8(c)). The fracture surface of the disordered 750-60 sample comprises coarse dimples next to the cavities demonstrating an entirely ductile mode of failure (Fig. 8(d)).

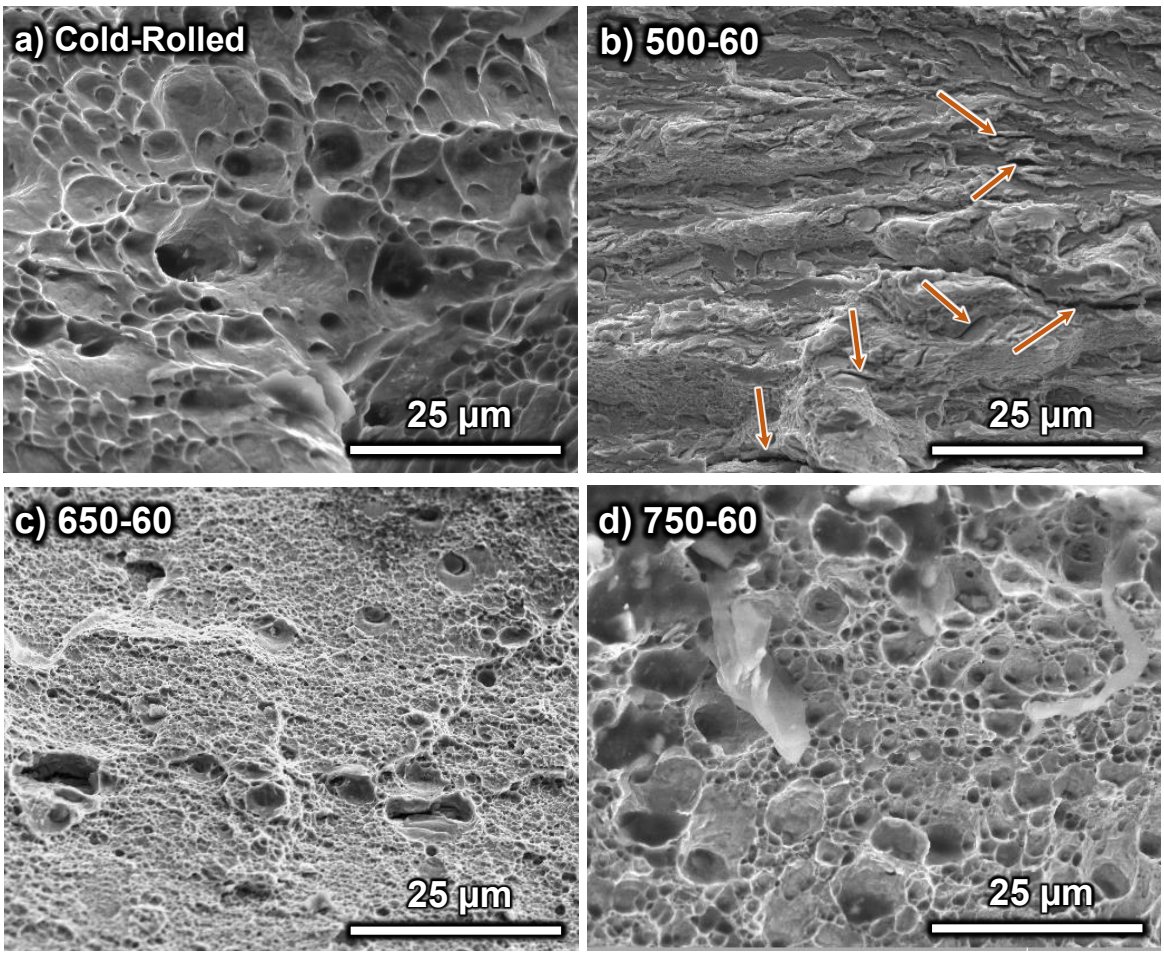

Fig. 8. SEM micrographs of fracture surface after tensile tests of a cold-rolled sample (a) and samples annealed at various temperatures for 60 min (b, c, and d).

4. Discussion

In the following, the experimental results of mechanical properties will be related to the evolutions of ordering and microstructure. Also, comparisons with earlier suggestions in the literature are given. Finally, the optimal combination of mechanical and magnetic properties will be presented and the annealing treatment for obtaining these properties will be suggested.

4.1. Analysis of the hardness changes

According to Fig. 5, the hardness of the samples varies depending on annealing temperature and holding duration. The reasons behind the hardness change can be determined by analyzing the process characteristics. The kinetics of many physicochemical reactions can be described by the Avrami / Kolmogorov-Johnson-Mehl-Avrami (KJMA) equation, where the Avrami exponent and the activation energy are two characteristics of the process. As explained in section 3.1, at low annealing temperatures, no changes in microstructure take place, so it can be assumed that the increase in the hardness observed after low annealing temperatures is only connected to the occurrence of the ordering transformation [3]. Therefore, it is possible to determine the characteristics of the ordering transformation for the present alloy. Recently, the long range ordering process in a Ni-Cr alloy was analyzed by Young et al. [19] using the microhardness data fitted with the KJMA equation.

The hardness changes after annealing at temperatures 300–600 °C were analyzed. The data in Fig. 5 and Table 1 from 310 HV up to 808 HV were fitted with the KJMA equation as follows:

$$f = (HV - HV_0) / (HV_{max} - HV_0) \quad (1)$$

$$f = 1 - \exp(-kt^n) \quad (2)$$

$$k = k_0 \exp(-Q/RT) \quad (3)$$

$$t_f = A \exp(Q/RT) \quad (4)$$

where f is the fractional change of the hardness and HV, HV_0 and HV_{max} are hardness values after a certain annealing condition, initial hardness before any annealing treatment, and the maximum hardness achieved through this process, respectively. k (rate constant) and k_0 (pre-exponential factor) are constants, R is the universal gas constant, T and t are the annealing temperature (K) and time (s) respectively. Q and n are the activation energy of the process and Avrami exponent respectively. The time t_f required for the progress of a certain fraction (f) is also dependent on Q and T, A being a constant, as expressed in Equation (4).

Vickers hardness data for annealing at the temperature range 300–600 °C and the fractional changes according to Equation 1 are presented in Tables 1 and 2, respectively. By plotting the relative change of the hardness (Table 2) as a function of the soaking time at each annealing temperature, the times required for a certain fraction (t_f) can be obtained. In order to fit the suitable curve on the existing data, the Avrami exponent n was estimated by linear regression of Log. (ln(1/(1-f))) vs. Log. (t) curves at various annealing temperatures from the slope of the fitted lines illustrated in Fig. 9. It is seen that the n only varies in the range of 0.30–0.36 which value is slightly lower than the same exponent for recrystallization of the present alloy, determined to be 0.4 [2]. There are no values of n reported in the literature for the ordering process in Fe-Co or Fe-Co-V alloys. Young et al. [19] obtained a somewhat higher value, n ≈ 0.63, for a Ni-Cr alloy.

Using these exponents, curves were fitted with the data, as demonstrated in Fig. 10. Afterward, the t_f for fractions of 50, 60, and 80 % at four annealing temperatures of 400, 450, 500, and 550 °C were predicted, and the values are listed in Table 3. By plotting ln(t_f) as a

function of 1/T (Fig. 11), the slope of the lines gives the value of Q/R (Equation (4)) for the fractions. These values and the obtained activation energy of Q are listed in Table 4. It is seen that the values of the activation energy Q are in the range of 132–144 kJ/mol. No values can be found in the literature for the 10%V alloy, but Sourmail [13] has listed Q as 154–170 kJ/mol (only one exceptional value 255 kJ/mol) for the long-range ordering process in Fe-Co and Fe-Co-2V alloys, determined by XRD based on the long-range order parameter. Besides, values of 105 kJ/mol and 170 kJ/mol were reported by Rajkovic and Buckley [20] for the activation energies of discontinuous and continuous ordering transformation respectively in Fe-50Co alloys containing less than 1%V. Thus, the present values are consistently in the same ranges confirming that the ordering is the process causing the hardness increase at low annealing temperatures, and the V content does not affect the activation energy value significantly. The Q is lower than the activation energy of self-diffusion, presumably affected by severe cold deformation of martensite increasing the dislocation density before the annealing.

Table 1. The hardness of annealed samples under various cycles

Annealing time (min)	Annealing temperature (°C)					
	300	400	450	500	550	600
10	335	411	506	584	634	747
30	352	446	564	628	678	808
60	365	464	608	690	751	770
120	390	514	660	721	761	680
240	405	564	680	740	715	545

Table 2. Fractional changes of the hardness according to equation 1

Annealing time (min)	Annealing temperature (°C)

	300	400	450	500	550	600
10	0.05	0.20	0.39	0.55	0.65	0.88
30	0.08	0.27	0.51	0.64	0.74	1
60	0.11	0.31	0.60	0.76	0.88	0.92
120	0.16	0.41	0.70	0.82	0.90	0.74
240	0.19	0.51	0.74	0.86	0.81	0.47

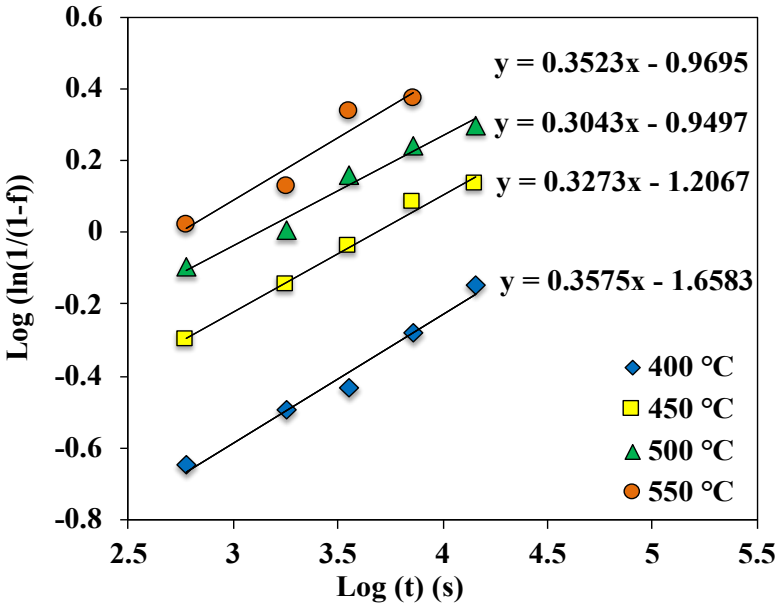

Fig. 9. Variations of *Log. (ln(1/(1-f)))* vs. *Log. (t)* for the Avrami exponent n.

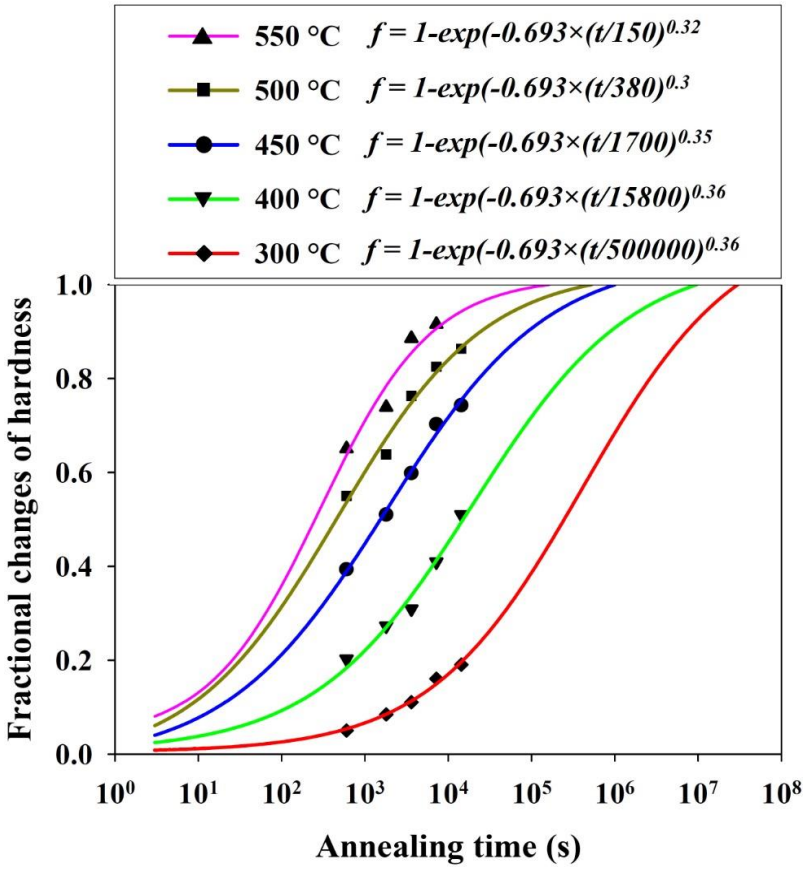

Fig. 10. Fractional changes of hardness as a function of annealing time at different temperatures and fitted equations.

Table 3. Required time (s) for 50%, 60%, and 80% relative hardness change predicted from equations in Fig. 10.

Annealing temperature (K)	Process progress time (s)		
	t_{50}	t_{60}	t_{80}
673	15800	34200	164000
723	1700	3780	18800
773	380	960	6300
823	150	360	2080

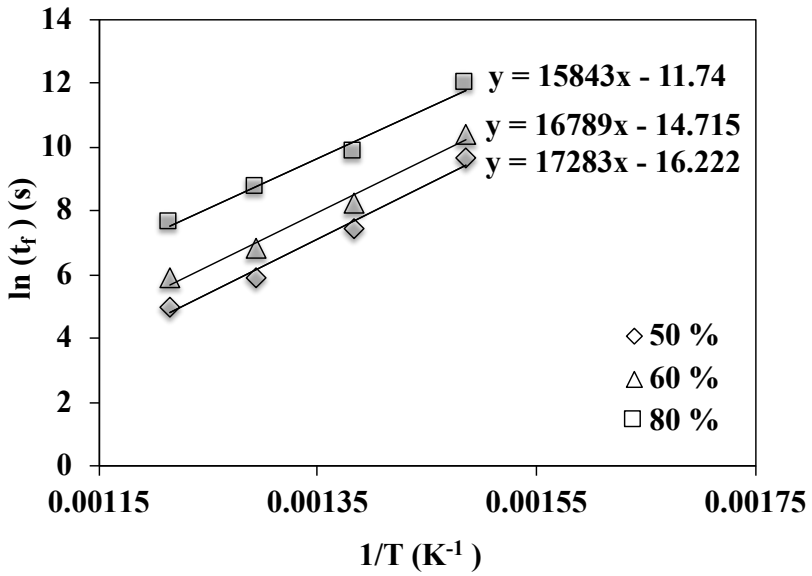

Fig. 11. Variation of *ln (t_f)* vs. inverse annealing temperature.

Table 4. Calculated values of the activation energy according to equation 4

Fraction (%)	Q/R (kJ/K^{-1})	Q (kJ/mol)
50	17283	143691
60	16789	139584
80	15843	131719

4.2. Hardness and microstructural evolution

The analysis of the kinetics of the hardness changes due to low-temperature annealing confirmed that the ordering process can explain these changes. This is expected because according to microstructural characterizations reported in Refs. [2,3], only the ordering transition can occur at low temperatures below 550 °C. The start of the ordering was detected at about 350 °C by dilatometry (Fig. 2(a)). As seen in Fig. 2(b), the superlattice reflection in XRD patterns indicates an intensification of the order up to 600 °C followed by weakening and vanishing towards higher temperatures.

There are very limited investigations concerning the correlation between hardness changes and degree of order in Fe-Co-V based alloys. Zakharov et al. [21] observed the highest hardness after annealing an Fe-52Co-6.85V alloy at 620 °C for 30 min which was in the temperature interval of ordering transformation. Consistently, Hasani et al. [14] reported an increase of hardness in an Fe-49.6Co-7.15V alloy after annealing at temperatures 200–550 °C (30 min) corresponding to the partially ordered condition.

At annealing temperatures above 500 °C, the rate of increase in hardness decreases, and even prolong holding times leads to a drop of hardness, which means that other processes are activating. As shown in Figs. 2(c,d), γ_2 precipitation and austenite transformation become evident concurrently at 550 °C. Precipitation hardening has been reported by some authors to be the only contributor responsible for hardness increment in Fe-Co-X ternary alloys especially at 600 °C [22,23]. However, it is obvious that increasing the hardness by annealing until 500 °C is not concerned with the precipitation, but due to the ordering transition. The softening of an Fe-40Co-5V-0.005B-0.015C-0.5Mo-0.5Nb (at.%) alloy after annealing treatments longer than 1 h at 600 °C was simply attributed to the over-aging condition [23]. According to our previous work [3], low-temperature austenite formed in the present alloy concurrently with $(Co,Fe)_3V$ precipitates during annealing at 550 °C and above, while this austenite remains stable during cooling down to room temperature due to vanadium enrichment (Fig. 4). It seems that the role of austenite transformation has not been accounted in previous studies as a softening process. Further, it was demonstrated that the austenite grains grow and consume rod-shaped γ_2 precipitates or precipitates themselves coalescence together and convert to austenite during prolonged annealing, causing reduction of the precipitates fraction, which might cause softening [3]. Besides, recovery in ferrite, which becomes evident at 550 °C and above [2], can also result in softening. However, a separate assessment of the effect of each phenomenon on hardness is not possible.

By annealing above the T_c (at 750 °C and above), the austenite formation is accelerated significantly (Fig. 3(c)) whereas the ordered state is vanished [11,24,25], while both of them lead to a steep drop in hardness values between 700 and 750 °C, evident in Fig. 5. The amount of austenite formed at 750 °C was doubled compared to that formed at 700 °C [3]. A slight increase in hardness after 4 h annealing at 750 °C can be attributed to martensite transformation during cooling due to reduction of austenite stability, imposed by austenite grain growth [3]. After annealing at 800 °C, the amount of martensite still increases that may be seen as a small hardness peak at this temperature. After annealing at temperatures ≥850 °C, the structure at room temperature is fully martensitic and the hardness remains practically constant with a very slight decreasing trend owing to grain growth [3].

4.3. Yield strength and YS/HV ratio

Variations of the YS due to the annealing of cold-rolled Fe-Co based alloys have been the subject of the number of studies so far [9,10,15,24,26,27], especially based on the relation between YS and the degree of order as well as ferrite grain size. Stoloff and Davies [9,11] studied the relation between the degree of order and YS in an Fe-Co-2V alloy and found that the YS exhibited a peak around an intermediate degree of order, slightly below the critical temperature T_c.

According to the present tensile tests (Fig. 7(a)), the YS of the cold-rolled alloy increased almost double by annealing at temperatures 300–450 °C; slightly more with longer holding times; in the range in which only the ordering process is activated. However, in annealing at higher temperatures, even in the ordered state below 730 °C, YS decreased. A steep drop after annealing at 750 °C is observed, where a constant YS level of about 800 MPa has reached, about half of the YS of the cold-rolled sheet.

Above annealing temperatures of 600 °C, a deep drop of YS can be attributed to various processes, including reduction of the degree of the order, increasing the amount of austenite as a soft fcc phase, decreasing the volume fraction of precipitates, and softening of ferrite through the recovery and recrystallization process. The distinction of the contributions of each mechanism on YS variations would be quite difficult. After annealing at 800 °C and above, the YS of the new martensite (with a small fraction of recrystallized ferrite at 800 °C) is recorded, so YS stays quite constant independent of annealing temperature and holding time.

Hardness test is frequently employed to predict other mechanical properties including YS and tensile strength [28,29] due to lower cost and easier and faster performance. Many studies have revealed that there is a linear relationship between hardness and YS [30–32]. For instance, Pavlina and Van Tyne [32], compiling strength-hardness data from the literature for various steels having the YS ranging widely from 325 to 1700 MPa, found the YS/HV ratio around 2.9. The YS means the start of tensile plastic yielding whereas the hardness indentation measures the resistance to compressive stress after significant plastic strain, thereby including the strain hardening phenomenon. The physical meaning of this ratio may be unclear, but its changes would reflect changes in strain hardening behavior, i.e., changes in deformation mechanism.

In the present results, consistently with the YS variations (Fig. 7(a)), the Vickers-hardness was seen to change during annealing (Fig. 5). The ratio of YS/HV after various annealing cycles was predicted and the values are plotted in Fig. 12. In addition to the data points, the variation of the arithmetic mean of the ratio at each temperature is shown by a curve. From the curve, it is seen that the ratio has a constant high value of about 4.5 after annealing at the lowest temperatures but it decreases to around 3.5 due to annealing at temperatures 500–600

°C. Then it rises abruptly back to about 4.5 after annealing at 650–700 °C and finally drops to a low level of about 3.5 due to annealing at higher temperatures.

It seems that the YS/HV ratio is distinctly higher than generally for steels, except after annealing in the temperature range of 500–600 °C and after annealing at the highest temperatures, i.e., 800 °C and above. In the narrow range of 500–600 °C, as a matter of fact, the fracture mode was brittle, so the ratio is the fracture stress/hardness, and the fracture stress is lower than what YS would be. However, without any deeper investigation, it is difficult to explain quantitatively the dependence of the fracture stress on annealing temperature (on the microstructure and ordering state). Anyhow, according to XRD results, the ordering continues above 450 °C reaching its maximum value at 600 °C. This intensifying order might be a reason for further embrittlement of the structure by reducing the tensile fracture stress. In hardness testing, however, compressive plastic strain takes place around the indent without fracture, and the flow resistance to compressive strain would be increased by increasing the degree of order. Thus, the low values of the ratio of fracture stress/hardness in this intermediate temperature range might result from this. The value is also dependent on holding time, decreasing with prolonged holding.

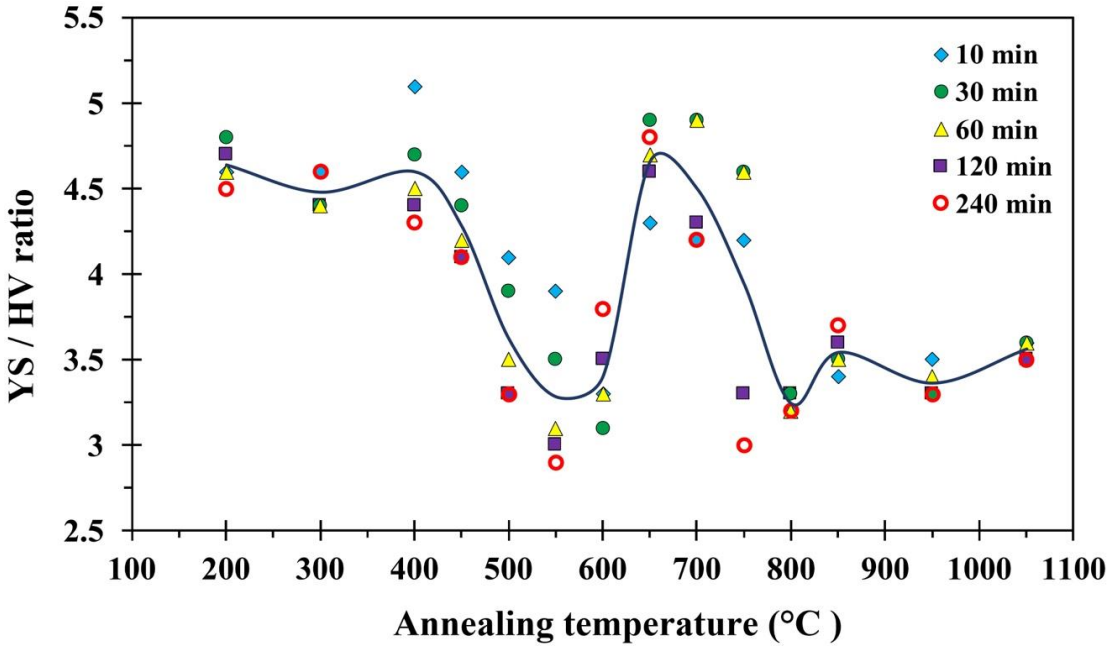

Fig. 12. The YS/HV ratio as a function of annealing temperature for various holding times. The curve shows the mean of the ratio at each temperature.

Notably, the YS/HV ratio has again a level of about 4.5 following annealing at 650–700 °C before it finally drops to almost a constant low level of around 3.5. If we exclude the range of brittle failure at 450–600 °C assuming that the ratio is there low due to fracture stress, it seems that the YS/HV ratio is about 4.5 after annealing at temperatures below 750 °C and about 3.5 after annealing at higher temperatures. This might be explained that in the ordered structure, inherited by annealing below about 730 °C, the work hardening is low and consequently HV value remains relatively low. However, for annealing temperatures at and above 800 °C, where the disordered state exists and the microstructure is martensitic after cooling, the stronger work hardening would occur, affecting the hardness value and thereby tending to decrease YS/HV. At 750 °C and to some extent also at 500–550 °C, the ratio is strongly dependent on the holding time being still high after a short holding but low after a long holding (120–240 min). At 600 °C, the inverse dependence exists concerning the increase of the ratio. The corresponding influence of the holding time is also evident in

stress-strain behavior, revealing the distinct changes in strain hardening behavior in the ferritic-austenitic microstructure depending on the progress of microstructure evolution. The strain hardening rate curves are, however, not shown here. As seen in Fig. 6(c), in tensile straining, discontinuous yielding takes place and the Lüders strain without any strain hardening is about 4% after 120 min annealing, but Lüders strain is more than 10% after 60 min holding (the curve not shown here). The complex details of plastic straining behavior related to the progress of microstructure evolution after annealing at 500–750 °C will be reported in a separate paper.

4.4. Ductility behavior

As clearly seen from Fig. 7(b), ductility decreased down to a zero level at low annealing temperatures below 600 °C for all soaking times, obviously as a result of the progress of the degree of order. It should be noted that a high fraction of γ_2 precipitates may also intensify the brittleness at 550 °C through the precipitation hardening effect [22,23]. However, as demonstrated above, the ordering process seems to be the controlling phenomenon in hardness increase up to an annealing temperature of 550 °C. By annealing at 600 °C, where the degree of order reaches its maximum (Fig. 2(b)), ductility starts to improve, which must be a result of austenite formation as well as initiation of recrystallization of ferrite [2,3,8,14]. At temperatures above 600 °C, the degree of order as well as fraction of precipitates decrease, so it can be concluded that their concomitant decrease, the progress of recrystallization, and increasing the volume fraction of retained austenite are the factors promoting the ductility.

After annealing at the temperature of 750 °C, where the superlattice reflection is absent as a sign of the disordered structure (Fig. 2(b)), and the highest amounts of austenite retain at room temperature and also the recrystallization makes remarkable progress, the ductility

reaches its maximum values for all soaking times. However, as can be noticed in Fig. 6(c), after annealing at 750 °C, the flow behavior with distinct discontinuous yielding is quite different from that after other annealing temperatures, which mostly concerns the amount and mechanical stability of the retained austenite, as will be discussed in a future publication. Annealing at 800 °C and above results in thermally unstable austenite that transforms to martensite upon cooling, decreasing the elongation, in spite of accomplishment of the recrystallization of ferrite and disordered state of the microstructure. To highlight and summarize the effects of the above-mentioned phenomena on the ductility, variations of all contributors, except the recrystallization, as a function of annealing temperature for 120 min soaking time are plotted in Fig. 13. Approximation of the degree of order was gained from the dilatometric run [3] as well as the XRD patterns.

Hasani et al. [33] observed the brittle tensile fracture mode in an Fe-49.6Co-7.15V alloy annealed at 700 °C. They concluded that the ductile mode would only happen in the disordered condition. A transition from a wavy glide of dislocations in the disordered condition to a planar glide on the ordered state was ascertained to be responsible for the embrittlement. However, in a contradict observation, the ductile mode of failure was seen in the present samples annealed at 650 °C (Fig. 8(c)) and 700 °C (not shown here) where the ordered state still existed. The reason for this manner in the present alloy can be attributed to the formation of a considerable amount of austenite (about 23 vol.% by annealing at 650 °C after 1 h) with very fine grain size (below 350 μm) along the ferrite grain boundaries, as displayed in Fig. 3(b). This austenite can prevent the grain boundary embrittlement causing the intergranular failure, typical in Fe-Co alloys as well as Fe-Co-V alloys in the ordered state [12,25,34]. In addition to the formation of austenite grains, grain refinement by the progress of recrystallization of ferrite can minimize the stress concentrations at grain boundaries [12].

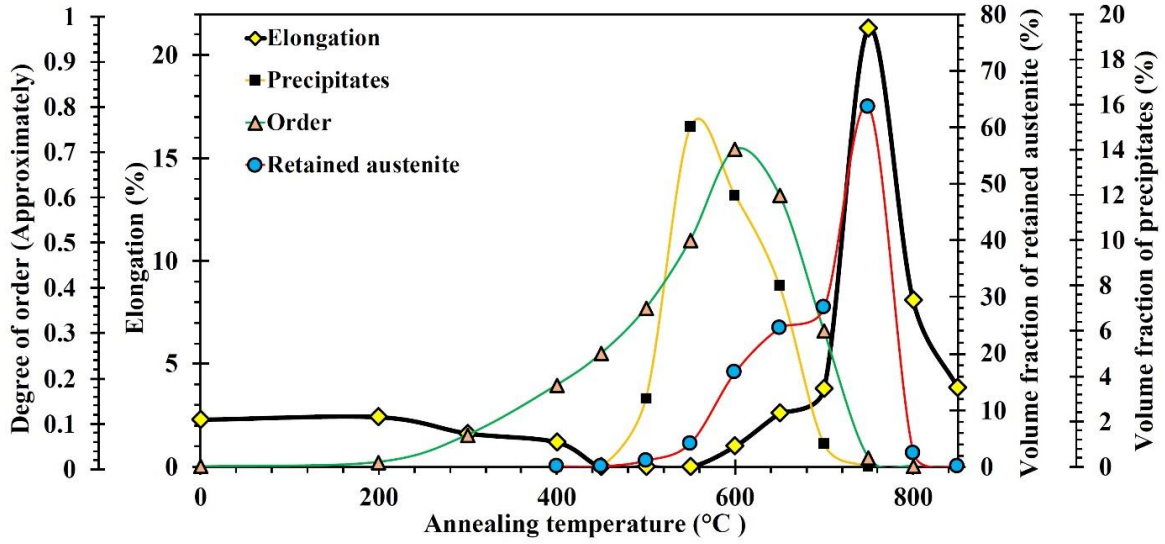

Fig. 13. Variations of ductility, the volume fraction of retained austenite and precipitates, and the approximate amount of degree of order after annealing at various temperatures for 120 min.

It has been already revealed that the recrystallization in the present alloy initiates after 60 min holding at 600 °C and proceeds with raising the annealing temperature and holding time [2]. Very fine recrystallized ferrite grains are formed at 650 °C (Fig. 3(b)), mostly along grain boundaries of initial ferrite, but no recrystallization at 500 °C yet. Therefore, both factors of austenite formation and progress of recrystallization which are taking place concurrently, prevent the grain boundary embrittlement and cleavage fracture. The annealing treatment at 750 °C, i.e., above T_c, at which the ordered state can no longer survive and a considerable amount of retained austenite is gained (about 65 vol.%) as shown in Fig. 3(c), in addition to the significant progress in recrystallization (about 89 %) [2], results in highest elongation and completely ductile failure.

4.5. Optimal annealing treatment

The present alloy is applied as semi-hard/ hard magnets in the industries, especially in high-speed motors, where the high coercive force (H_c) and remanence (M_r) as well as high YS and

adequate ductility of the material are required. According to the results of vibrating sample magnetometer analysis (discussed in Ref. [4]), the highest H_c was obtained after 60 min soaking at 600 °C (sample coded by 600-60). However, as evident from Fig. 14(a), the H_c after annealing at 650 °C for 10 min (650-10) is very close to that of the 600-60 sample. Furthermore, the amount of M_r of the 650-10 sample is slightly higher than that of the 600-60 sample which means that the magnetic properties of the alloy annealed under these two conditions are quite similar. On the other hand, according to Fig. 14(b), it is observed that although the YS of both samples is equal, the elongation of the 650-10 sample is better than that of the 600-60 sample. In order to identify the reasons for better elongation, the EBSD phase + high-angle grain boundary maps concern both conditions are presented in Figs. 14 (c,d). As seen, the fraction of austenite and its grain size for both conditions are quite similar. However, the recrystallization fraction, determined by the grain orientation spread (GOS) analysis [2], is higher in the microstructure of 650-10 sample. This is the most important reason for better elongation though decreasing the degree of order at 650 °C could be effective as well. Therefore, considering both the mechanical and magnetic properties, annealing for 10 min at 650 °C can be recommended as the optimal annealing treatment for the present alloy.

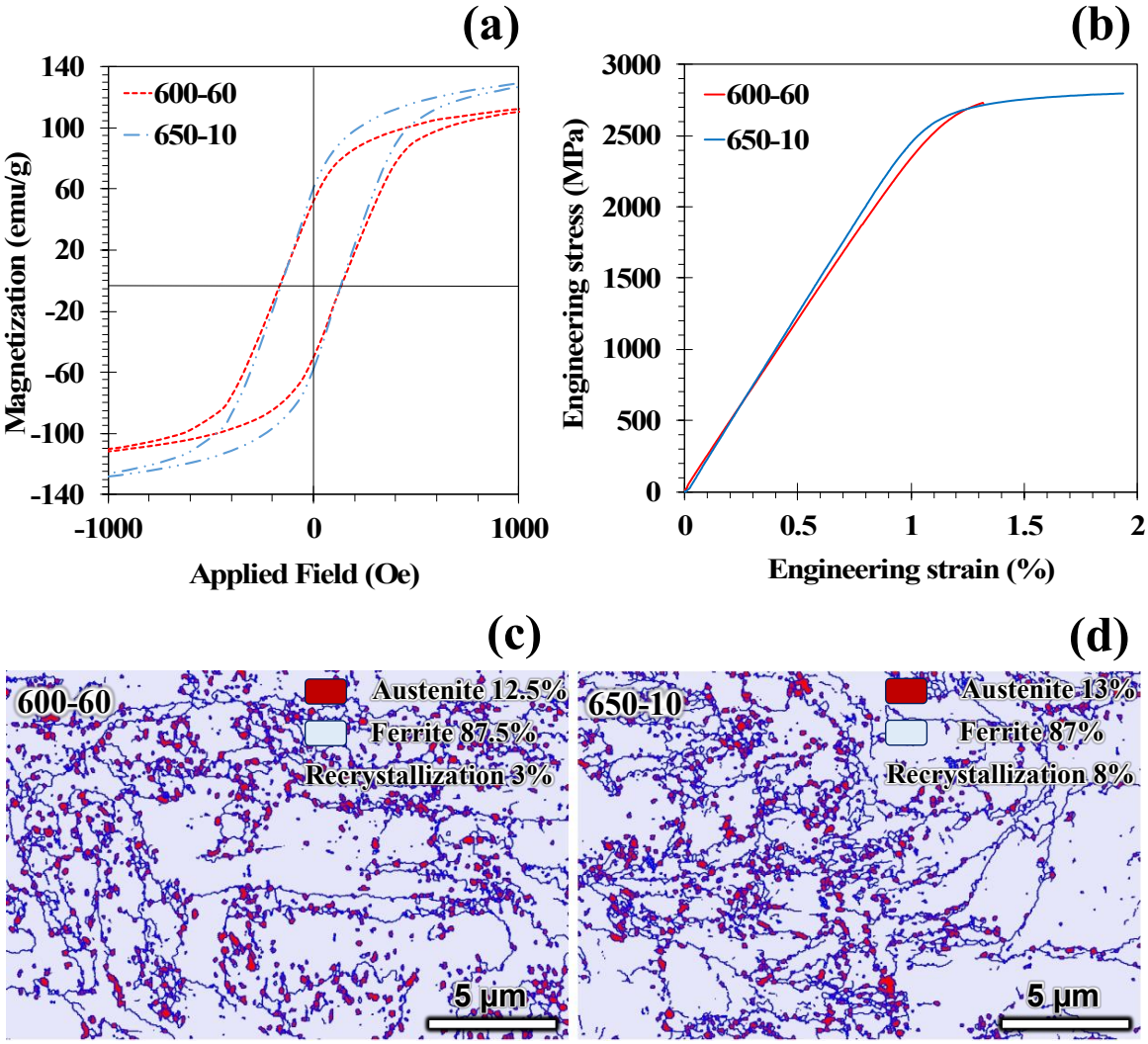

Fig. 14. Comparison of magnetic (a) and mechanical properties (b) and microstructures of the samples annealed at 600 °C for 60 min (c) and at 650 °C for 10 min (d).

5. Summary and conclusions

In this study, relationships between mechanical properties and ordering, recovery, recrystallization, and phase evolutions tacking place during annealing in an 86 % cold-rolled Fe-50Co-10V alloy were investigated. Annealing was carried out in the temperature range 200–1050 °C with the holding times between 10 to 240 min. Extended hardness as well as tensile tests were carried out at room temperature to investigate the dependence between

microstructure and mechanical properties. Based on the results, the main conclusions can be summarized as follows:

1- Hardness increased with increasing the annealing temperature and holding time due to annealing of the cold-rolled alloy at temperatures up to 550 °C. The peak hardness was obtained at 600 °C with a holding time of 30 min. At annealing temperatures above 600 °C, progress in recovery and recrystallization of ferrite, formation of a considerable amount of austenite, and reduction of the degree of order were obvious reasons for the lowering hardness.

2- The analysis of the kinetics of hardness changes up to annealing at 550 °C by the JMKA equation indicated that the hardness increase was controlled by the ordering process. The Avrami-exponent was found to be in the range 0.3–0.36 and the activation energy 132–144 kJ/mol, the latter being in good agreement with the existing data for the ordering process in Fe-Co and Fe-Co-2V alloys in the literature.

3- The YS increased during annealing at low temperatures up to 450 °C, reaching the maximum ≈ 2.7 GPa, while only the ordering transition occurred. At higher annealing temperatures, YS decreased due to brittle fracture in the temperature range of 450–550 °C. Above 600 °C, the formation of austenite which retained to room temperature together with the restoration of ferrite led to decreasing YS. A steep drop in YS was observed after annealing at 750 °C owing to the disordered state, fast softening of ferrite, and the formation of a high amount of austenite. After annealing at the highest temperatures of 800–1050 °C, the structure consisted of various fractions of recrystallized ferrite, retained austenite, and new martensite, with quite a constant YS of 0.9 GPa.

4- The ratio of YS/HV was high, around 4.5, after annealing at low temperatures, where the ordering was the controlling process. After annealing at high temperatures of 800–1050 °C where the structure consisted of various fractions of recrystallized ferrite, retained austenite, and new martensite, the ratio was distinctly lower, around 3.5. This difference is related to different strain hardening and ordering/disordering states of the microstructure.

5- Elongation decreased obviously as a result of increasing the degree of order and became nil after annealing in the temperature range 450–550 °C. By annealing at 600 °C and above, the elongation was improved owing to increasing the austenite fraction and progress of recovery and recrystallization. The maximum elongation was achieved by annealing at 750 °C due to the formation of the disordered state, significant recrystallization, and a considerable amount of properly metastable retained austenite.

6- Failure mode varied from ductile in the cold-rolled condition to the brittle mode after annealing at 500 °C. However, the ductile failure mode with fine dimples was observed after annealing at 650 °C, even though the ordered state still existed.

7- Annealing at 650 °C for 10 min can be recommended as the optimal annealing treatment for the present alloy providing the best combination of magnetic and mechanical properties.

Acknowledgments

M.R.K is grateful for financial support from the Iranian government for his research stay at the University of Oulu and for the facilities and equipment provided by the University of Oulu for performing this study. L.P.K, V.J, and J.K acknowledge the support of the Academy of Finland for the “Genome of Steel” project #311934.

Author’s contributions

Mohammad Reza Kamali designed and performed all experiments, analyzed the data, prepared figures, and wrote the main part of the draft manuscript. Ali Reza Mashreghi designed the experiments and supervised the project. Pentti Karjalainen supervised the study, contributed to discussions by commenting, drawing conclusions, and writing, checking, and revising the manuscript. Saeed Hasani supervised the project and designed the experiments. Vahid Javaheri participated in the preparation of some figures, commenting, and revising the manuscript. Mirtaher Seiyedbeigi participated by visualization and performing some experiments. Jukka Komi contributed to discussions by commenting and general supervising.

Declarations of interest: none.

Data availability

The raw/processed data required to reproduce these findings cannot be shared at this time due to technical or time limitations.

References

[1] B.T. Hailer, Effect of heat treatment on magnetic and mechanical properties of an iron-cobalt-vanadium-niobium alloy, Master's thesis, Virginia Polytechnic Institute, Blacksburg-Virginia, USA, 2001.

[2] M.R. Kamali, L.P. Karjalainen, A.R. Mashregi, S. Hasani, V. Javaheri, J. Kömi, Reobservations of ferrite recrystallization in a cold-rolled ordered Fe–50Co–10V alloy using the EBSD method, Mater. Charact. 158 (2019) 109962. doi:10.1016/j.matchar.2019.109962.

[3] M.R. Kamali, A.R. Mashreghi, L.P. Karjalainen, S. Hasani, V. Javaheri, S. Saukko, J. Kömi, Reobservations on ordering, precipitation and polymorphic phase

transformation phenomena during annealing of a severely cold rolled magnetic Fe-Co-10V alloy, Materialia. 12 (2020) 100765. doi:10.1016/j.mtla.2020.100765.

[4] M.R. Kamali, A.R. Mashreghi, L.P. Karjalainen, S. Hasani, V. Javaheri, J. Kömi, Influence of microstructure and texture evolution on magnetic properties attained by annealing of a cold-rolled Fe-Co-10V semi-hard magnetic alloy, Mater. Charact. (2020) 110591. doi:10.1016/j.matchar.2020.110591.

[5] R. Gilles, M. Hofmann, Y. Gao, F. Johnson, L. Iorio, M. Larsen, F. Liang, M. Hoelzel, B. Barbier, Probing the relationship of long-range order in nanodomain FeCo alloys with ternary additions using neutron diffraction, Metall. Mater. Trans. A. 41 (2010) 1144–1150. doi:10.1007/s11661-009-9933-y.

[6] P. Moine, J.P. Eymery, P. Grosbras, The effects of short-range order and long-range order on the equilibrium configuration of superdislocations in Fe-Co : 2 at% V — consequences on flow stress, Phys. Status Solidi. 46 (1971) 177–185. doi:10.1002/pssb.2220460115.

[7] M.J. Marcinkowski, H. Chessin, Relationship between flow stress and atomic order in the FeCo alloy, Philos. Mag. 10 (1964) 837–859. doi:10.1080/14786436408225388.

[8] B. Nabi, A. Helbert, F. Brisset, G. André, T. Waeckerlé, T. Baudin, Effect of recrystallization and degree of order on the magnetic and mechanical properties of soft magnetic FeCo–2V alloy, Mater. Sci. Eng. A. 578 (2013) 215–221. doi:10.1016/j.msea.2013.04.066.

[9] N.S. Stoloff, R.G. Davies, The mechanical properties of ordered alloys, Prog. Mater. Sci. 13 (1968) 1–84. doi:http://dx.doi.org/10.1016/0079-6425(68)90018-2.

[10] L. Ren, S. Basu, Y.U. R-Hai, J.Q. Xiao, A. Parvizi-Majidi, Mechanical properties of Fe-Co soft magnets, J. Mater. Sci. 36 (2001) 1451–1457. doi:10.1023/A:1017588411888.

[11] N.S. Stoloff, R.G. Davies, The plastic deformation of ordered FeCo and Fe3Al alloys, Acta Metall. 12 (1964) 473–485. doi:10.1016/0001-6160(64)90019-7.

[12] R.S. Sundar, S.C. Deevi, Effect of heat-treatment on the room temperature ductility of an ordered intermetallic Fe-Co-V alloy, Mater. Sci. Eng. A. 369 (2004) 164–169. doi:10.1016/j.msea.2003.11.004.

[13] T. Sourmail, Near equiatomic FeCo alloys: Constitution, mechanical and magnetic properties, Prog. Mater. Sci. 50 (2005) 816–880. doi:10.1016/j.pmatsci.2005.04.001.

[14] S. Hasani, M. Shamanian, A. Shafyei, M. Nezakat, H. Mostaan, J.A. Szpunar, Effect of recrystallization and phase transitions on the mechanical properties of semihard magnetic FeCo-7.15V alloy during the thermomechanical Process, Metall. Mater. Trans. A. 48 (2017) 1903–1909. doi:10.1007/s11661-017-3954-8.

[15] T. Sourmail, Evolution of strength and coercivity during annealing of FeCo based alloys, Scr. Mater. 51 (2004) 589–591. doi:10.1016/j.scriptamat.2004.05.028.

[16] D.R. Thornburg, High- strength high- ductility cobalt- iron alloys, J. Appl. Phys. 40 (1969) 1579–1580. doi:10.1063/1.1657779.

[17] R.S. Sundar, S.C. Deevi, Soft magnetic FeCo alloys: alloy development, processing, and properties, Int. Mater. Rev. 50 (2005) 157–192. doi:10.1179/174328005X14339.

[18] G.B. Chon, K. Shinoda, S. Suzuki, B. Jeyadevan, Order-disorder transformation in Fe50Co50 particles synthesized by polyol process, Mater. Trans. 51 (2010) 707–711. doi:10.2320/matertrans.M2009251.

[19] G.A. Young, J.D. Tucker, D.R. Eno, The kinetics of long range ordering in Ni-Cr and Ni-Cr-Fe alloys, 16th Annu. Conf. Environ. Assist. Crack. Mater. Nucl. Power Syst. - Water React. Asheville, NC, USA. (2013) 22.

[20] M. Rajkovic, R.A. Buckley, Ordering transformations in Fe-50Co based alloys, Met. Sci. 15 (1981) 21–29. doi:10.1179/msc.1981.15.1.21.

[21] V.M. Zakharov, M.A. Libman, E.I. Estrin, On the role of atomic ordering in the formation of a high-coercivity state in iron-cobalt-vanadium alloys, Phys. Met. Metallogr. 113 (2012) 43–47. doi:10.1134/s0031918x12010152.

[22] R.S. Sundar, S.C. Deevi, B.V. Reddy, High strength FeCo–V intermetallic alloy: electrical and magnetic properties, J. Mater. Res. 20 (2005) 1515–1522. doi:10.1557/JMR.2005.0206.

[23] R. Sundar, S. Deevi, Influence of alloying elements on the mechanical properties of FeCo–V alloys, Intermetallics. 12 (2004) 921–927. doi:10.1016/j.intermet.2004.02.022.

[24] A. Duckham, D. Zhang, D. Liang, V. Luzin, R. Cammarata, R. Leheny, C. Chien, T. Weihs, Temperature dependent mechanical properties of ultra-fine grained FeCo–2V, Acta Mater. 51 (2003) 4083–4093. doi:10.1016/S1359-6454(03)00228-3.

[25] J.F. Dinhut, J.P. Eymery, P. Moine, Plastic deformation and brittleness of Fe-Co-V, Phys. Status Solidi. 12 (1972) 153–161. doi:10.1002/pssa.2210120115.

[26] L. Zhao, I. Baker, The effect of grain size and Fe:Co ratio on the room temperature yielding of FeCo, Acta Metall. Mater. 42 (1994) 1953–1958. doi:10.1016/0956-7151(94)90020-5.

[27] B. Nabi, A. Helbert, F. Brisset, R. Batonnet, G. André, T. Waeckerlé, T. Baudin, Effect of long range order on mechanical properties of partially recrystallized Fe49Co–2V alloy, Mater. Sci. Eng. A. 592 (2014) 70–76. doi:10.1016/j.msea.2013.10.093.

[28] J.T. Busby, M.C. Hash, G.S. Was, The relationship between hardness and yield stress in irradiated austenitic and ferritic steels, J. Nucl. Mater. 336 (2005) 267–278. doi:10.1016/j.jnucmat.2004.09.024.

[29] J.R. Cahoon, W.H. Broughton, A.R. Kutzak, The determination of yield strength from hardness measurements, Metall. Trans. 2 (1971) 1979–1983.

doi:10.1007/BF02913433.

[30] M. Toloczko, G. Lucas, G. Odette, R. Stoller, M. Hamilton, An investigation of microstructures and yield strengths in irradiated austenitic stainless steels using small specimen techniques, in: Eff. Radiat. Mater. 17th Int. Symp., ASTM International, 100 Barr Harbor Drive, PO Box C700, West Conshohocken, PA 19428-2959, n.d.: pp. 902-902–17. doi:10.1520/STP16515S.

[31] M. Gasko, G. Rosenberg, Correlation between hardness and tensile properties in ultra-high strength dual phase steels, Mater. Eng. 18 (2011) 155–159. http://fstroj.uniza.sk/journal-mi/PDF/2011/27-2011.pdf.

[32] E.J. Pavlina, C.J. Van Tyne, Correlation of yield strength and tensile strength with hardness for steels, J. Mater. Eng. Perform. 17 (2008) 888–893. doi:10.1007/s11665-008-9225-5.

[33] S. Hasani, A. Shafyei, M. Nezakat, H. Mostaan, P. Behjati, P. Sahu, The effect of the order-disorder transition on the electrical, magnetic and mechanical properties of Vicalloy I, Intermetallics. 81 (2017) 73–79. doi:10.1016/j.intermet.2017.02.027.

[34] L. Zhao, I. Baker, The effect of grain size and Fe: Co ratio on the room temperature yielding of FeCo, Acta Metall. Mater. 42 (1994) 2–7. doi:10.1016/0956-7151(94)90020-5.